Low-field magnetoresistance in La$_{0.7}$Ca$_{0.3}$MnO$_3$ manganite compounds prepared by the spray drying technique

B. VERTRUYEN, A. RULMONT, R. CLOOTS
SUPRATECS, Chemistry Institute B6, University of Liege, B-4000 Liege, Belgium

J.-F. FAGNARD
SUPRATECS, Physics Institute B5, University of Liege, B-4000 Liege, Belgium

M. AUSLOOS
SUPRATECS, Montefiore Institute B28, University of Liege, B-4000 Liege, Belgium

I. VANDRIESSCHE, S. HOSTE
Department of Inorganic and Physical Chemistry, Ghent University, Krijgslaan 281-S3, B-9000 Gent, Belgium

Abstract

Calcium-substituted lanthanum manganite compounds were synthesized by the spray drying technique. This method—whose main advantages are versatility, high reproducibility and scalability—yields small grain materials of high homogeneity and displaying low-field magnetoresistance effects. We report about the physical and chemical characterizations of these samples in order to investigate the potential interest of spray drying for the production of materials for low-field magnetoresistance applications. We have studied the dependence of the low-field magnetoresistance on the temperature and duration of the thermal treatment applied to the pelletized powders. The issue of the shape anisotropy (demagnetisation effects) influence on the magnetoresistance properties has also been dealt with.

1. INTRODUCTION

Since the early nineties, there has been a renewed interest in the mixed-valence manganites Ln$_{1-x}$A$_x$MnO$_3$ (where Ln is a lanthanide cation and A is often an alkaline earth ion), due to the discovery of their colossal magnetoresistance (CMR) [1-3]. Such materials have various potential applications, e.g., as magnetic sensors or in computer memory systems [4]. The physical properties of these compounds are influenced by several parameters [5, 6]. The chemical composition mainly affects the magnetic behaviour and the magnetic and electrical transition temperatures [5, 7]. The microstructure of the material can also have a strong influence on the physical properties, as proven by comparative studies of thin films, bulk ceramics and single crystals [8-11]. On one hand, the magnetoresistance of single crystals and epitaxial thin films is quite large but concentrated within a narrow temperature range around the Curie temperature T_C [8]. On the other hand, polycrystalline materials—either bulk ceramics or thin films—display a significant magnetoresistance at low fields and all temperatures below Tc, turning them into promising candidates for technical applications [12-14].

The most pronounced low-field effects are usually observed in samples characterized by a small grain size, typically less than 1 μm [12]. Such materials cannot be obtained by the usual solid state reaction technique [15]. Low-temperature precursor methods are used, for example co-precipitation [16], sol-gel [17] or combustion [18]. However the optimisation of these synthesis routes is time-consuming, due to the large number of experimental parameters to be controlled. Besides, these methods are generally not appropriate when large quantities of the product are needed.

In this study, we report about the synthesis of manganite compounds by the spray drying technique [19]. In this method, an aqueous solution of the metallic cations is sprayed into droplets, which are dried by a hot air flow. The main advantages of this method are its simplicity, reproducibility and versatility: there are only a few experimental parameters, which usually do not need to be modified when the chemical composition is changed. In addition, the grain size of the powders obtained can be controlled through concentration of the sprayed solution and final inhomogeneity in the powders is limited by the size of the sprayed droplets and is usually of nanometric scale. Moreover, spray drying is both a laboratory-scale method and an industrial processing technique: the same principles apply, only the dimension of the apparatus changes. Therefore spray drying might

be a promising technique for the preparation of small grain materials exhibiting low-field magnetoresistance effects.

2. EXPERIMENTAL

$La_{0.7}Ca_{0.3}MnO_3$ samples were synthesized from precursor powders obtained by the spray drying technique. The aqueous feedstock solution was prepared by dissolving stoichiometric amounts of La_2O_3, $CaCO_3$ and manganese acetate with a minimal amount of acetic acid. The total metallic cation concentration ([La] + [Ca] + [Mn]) was approximately 0.85 mol/l. The pH of the solution (~6) was found suitable for the spray drying process, since too acid solutions may damage the metallic parts of the spray drying apparatus such as nozzles or protective coatings in the cyclone [19].

Spray drying was performed through a co-current flow atomisation process in a Büchi B-191 apparatus using a 0.7 mm nozzle. The inlet temperature was 200°C. The liquid feed rate was 5 ml/min. The spray drying was carried out in air, using a flow rate of 600 normal 1/h. The outlet temperature during spraying was 135°C.

After spray drying, the powder was heated in air at 350°C for 2 h and at 600°C for 5 h in platinum crucibles. A slow heating rate (10°C/h) was used in the temperature range (200-350°C) corresponding to the main gaseous release as determined from thermal analysis. This precursor powder was then pressed uniaxially into 13 mm diameter pellets and submitted to different thermal treatments in platinum crucibles. The labels and thermal treatments of the samples whose properties are discussed in the following can be found in Table I. A letter "*b*" in the sample identification indicates a thermal treatment exceeding 2 h.

The samples were characterised by various techniques. X-ray diffraction was performed with a Siemens D5000 diffractometer (Cu KA, radiation). Thermogravimetric Analysis (TGA) and Differential Scanning Calorimetry (DSC) were carried out in a Netzsch STA449C apparatus. Fourier transform infrared (FTIR) spectroscopy was performed on powders dispersed in KBr disks. The morphology of the samples was studied by scanning electron microscopy using a Philips XL30 FEG-ESEM. The cationic composition was checked by Energy Dispersive X-ray Analysis (EDAX system). The physical properties were measured as a function of temperature and magnetic field using a Quantum Design PPMS (electrical resistivity measurements) and an Oxford Instruments VSM (magnetic moment measurements).

TABLE I : *Final thermal treatment (heating rate 150°/h), temperature of the resistivity maximum (under 0 T) and electrical resistivity at 20 K (under 0 T) for all samples discussed in this paper*

Sample	Final thermal treatment	$T_{\rho peak}$ (K), 0 T	$\rho(\Omega.cm)$ 20 K, 0 T
S 800	800°C during 2h	_	_
S 800b	800°C during 48 h	170	1.5767
S900	900°C during 2h	193	0.8135
S900b	900°C during 24 h	213	0.3761
S1000	1000°C during 2 h	230	0.1306
S1100	1100°C during 2h	266	0.0153
S1200	1200°C during 2 h	268	3.4×10^{-3}
S 1250b	1250°C during 5 h	267	2.1×10^{-3}

Figure 1: *Thermal analysis of the as-sprayed powder: weight loss (plain line) and DSC signal (dashed line).*
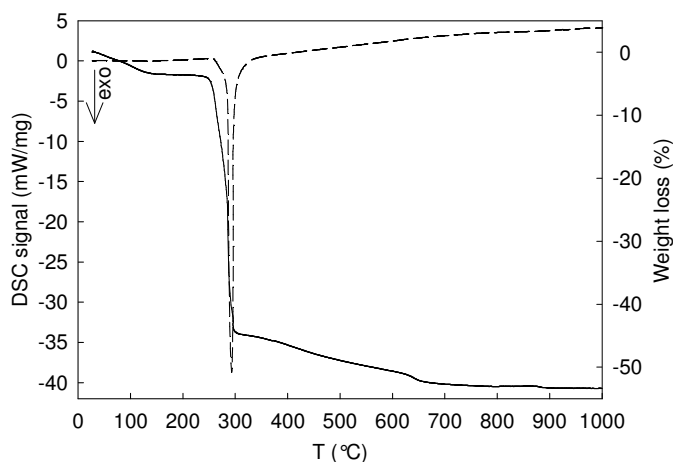

3. RESULTS AND DISCUSSION

The as-sprayed powder was found to be amorphous by X-ray diffraction. Based on IR spectroscopy and thermogravimetric analysis, it could be demonstrated that the powder only contained acetates of the different metallic cations. Fig. 1 displays the thermal analysis of the as-sprayed powder, carried out in air at 5°C/min. The main weight loss, characterised by a sharp exothermic peak, occurs around 280°C. The subsequent weight loss corresponds to the sluggish decomposition of the lanthanum oxycarbonate $La_2O_2CO_3$ formed during the first step of the heating process. This salt is frequently encountered during low-temperature synthesis of lanthanum compounds using carbonaceous precursors [20, 21]. This is why nitrate salts should be preferred whenever possible. However, preliminary tests with nitrates had shown that the sprayed product is too hygroscopic to be collected.

The samples prepared by the different thermal treatments (see Table I) were characterised by X-ray diffraction. A few diffractograms are shown in Fig. 2. The S800 sample contains both lanthanum oxycarbonate and the perovskite manganite phase (diffractogram a). The secondary phase is not detected in the case of the S900 sample (diffractogram b): this indicates that a 2 h thermal treatment requires a minimum temperature of 900°C. However single-phase materials can be obtained at lower temperatures if the duration of the treatment is increased, as shown by diffractogram c for the S800b sample sintered during 48 h. Diffractogram d is for the S 1250b sample: the sharpness of the perovskite reflections confirms that increasing the temperature and/or duration of the thermal treatment leads to an improved crystallisation of the final product.

The microstructure of the samples was studied by scanning electron microscopy. Fig. 3a illustrates the typical spherical shape of the particles obtained immediately after spray drying. Nucleation of the grains occurs during the thermal treatment at 600°C, yielding small grains of about 50 nm (Fig. 3b). Increasing the temperature of the subsequent thermal treatment leads to (i) an increase of the mean grain size and (ii) a better connectivity between the grains, as shown by the Fig. 3c and d for samples S900 and S1200 respectively. All samples studied here display a resistive transition from a metallic-like state at low temperature to an insulating state at high temperature. The temperature of the resistivity transitions are summarised in Table I. The transition temperatures of the samples prepared at 1100°C or higher temperature are in agreement with what could be expected for a chemical composition $La_{0.7}Ca_{0.3}MnO_3$, i.e., about 265 K [6]. Lower transition temperatures are observed for samples prepared at temperatures below 1100°C: decreasing the temperature of the thermal treatment leads to a lower transition temperature and also to a smaller grain size (see the microstructure results). Such a behaviour has been observed and discussed by several authors [22-24]. Briefly, these phenomena can be related to issues such as poor crystallinity [12, 22] and high surface/volume ratio resulting from a small grain size [24, 25].

Figure 2: *X-ray diffraction patterns of samples: (a) S800, (b) S900, (c) S 800b, and (d) S 1250b. Circles* (o) *indicate the reflections of the manganite phase, asterisks (*) indicate the reflections of the lanthanum oxycarbonate phase (La$_2$O$_2$CO$_3$, JCPDS 48-1113).*
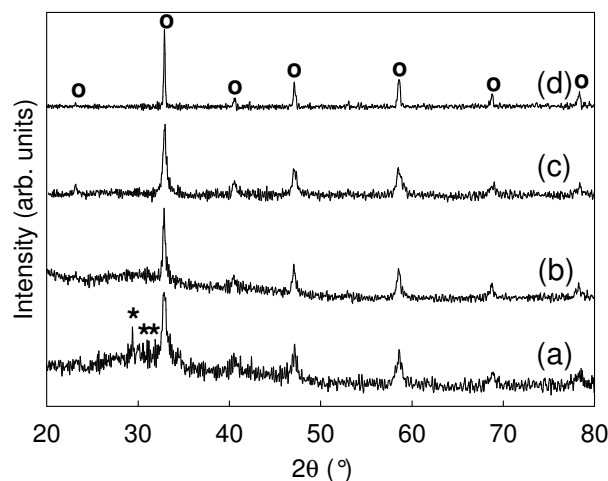
The last column in Table I displays the electrical resistivity values at 20 K without applied magnetic field. It can be seen that the resistivity decreases when the temperature or the duration of the thermal treatment is increased: the highest resistivity values are observed for the samples with the smallest grain sizes and the poorest connectivities. This is coherent with results from the literature, where the low temperature resistance of manganite compounds was shown to depend on the microstructure of the material: comparative studies of thin films, polycrystalline bulk ceramics and single crystals indicate that the presence of grain boundaries drastically increases the resistance at low temperature [8-10]. The physical mechanism responsible for this feature is still a matter of debate (scattering [26], spin-dependent tunnelling [27], mesoscopic model [28]) but the common idea of these models is that the propagation of the charge carriers is hindered at the grain boundary.

The electrical resistance properties of manganite compounds can be strongly modified by the application of a magnetic field. All the samples discussed in this paper display a qualitatively similar behaviour, with a sharp decrease of the resistance at low field and a smoother dependence for higher fields, as illustrated in Fig. 4 in the case of the S1100 sample: inset (a) shows the dependence of the *R/R(0)* ratio (where *R(0)* is the electrical resistance under zero magnetic field) as a function of the applied magnetic field H_a at 20 K, for two orientations of the magnetic field with respect to the long axis of the sample (6.9 x 1.85 x 0.9 mm^3). It can be seen that the applied magnetic field corresponding to the transition from the low-field to the high-field behaviour depends on the orientation of the applied magnetic field with respect to the parallelepipedic shape of the sample.

Since the samples studied here are poly-crystalline, the only cause for this anisotropy should be *shape-dependent* anisotropy, i.e., demagnetisation effects, which depend on the geometry of the sample. In order to examine this point, the data have to be plotted as a function of the *internal* magnetic field. If the orientation dependence is only due to shape anisotropy, the two sets of data should coincide.

Using the classical notations, the internal magnetic field H_i is given by $H_a - D \cdot M$, where H_a and M respectively denote the applied field and the sample magnetisation; D is the demagnetisation factor ($0 < D < 1$). The magnetic moment data (see inset (b) of Fig. 4) were converted to magnetisation values using the density (4,8) calculated from the molar mass (212.2g/mol), the crystallographic cell volume (230,9 Å^3) and the apparent density (79%) determined by the Archimedes' method. The D value for the parallel orientation (i.e., magnetic field applied parallel to the long axis of the sample) was estimated from the sample dimensions [29] to be about 0.05. For the perpendicular orientation (i.e., magnetic field perpendicular to the long axis of the sample), a D value of 0.51 was experimentally determined from the low field slope of the magnetic moment vs. H_a curve [30]. Finally the *R/R(0)* data could be plotted as a function of the internal magnetic field (main Fig. 4): the curves for the two orientations match remarkably well, considering the limited accuracy in the determination of the D values.

From the above discussion it can be concluded that the applied magnetic field corresponding to the transition from the low-field to the high-field behaviour strongly depends on the geometry of the sample and cannot be considered as an intrinsic property of the material. Incidentally, this means that the slope of the low-field magnetoresistance can be modified simply by changing the geometry of the sample.

Figure 3: *Scanning electron micrographies of: (a) as-sprayed powder, (b) powder heated to 600°C, (c) S900 sample, and (d) S1200 sample.*
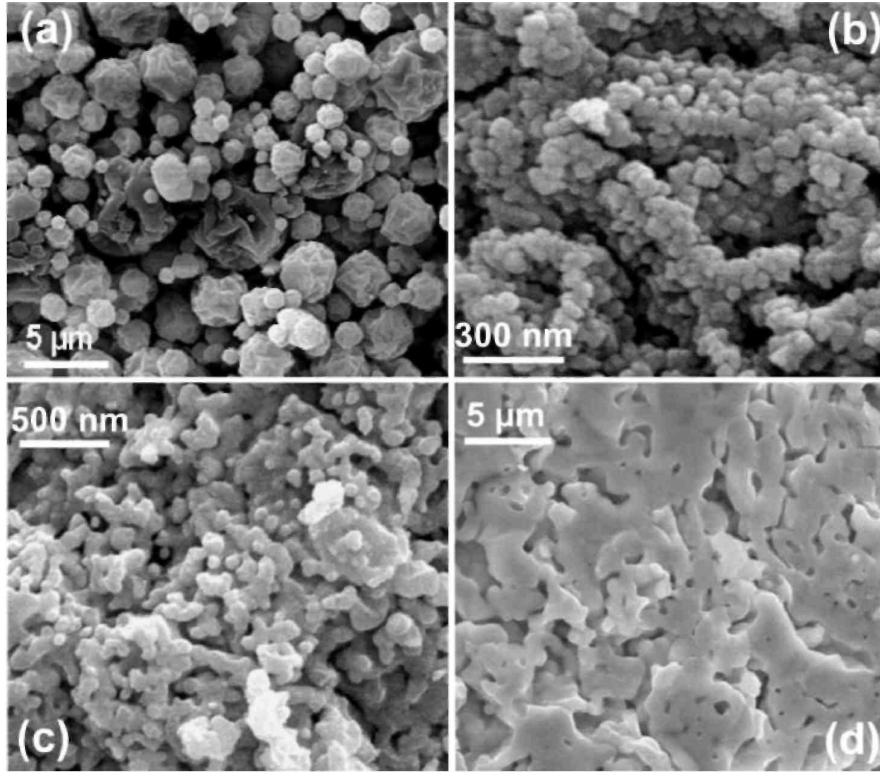
Figure 4: *Physical properties of the sample S1100 at 20 K. Inset (a) and (b): R/R(0) ratio (a) and magnetic moment (b) as a function of the applied magnetic field for parallel (black symbols) or perpendicular (white symbols) orientation of the magnetic field with respect to the long axis of the sample. Main figure: Same data plotted as a function of the internal magnetic field.*
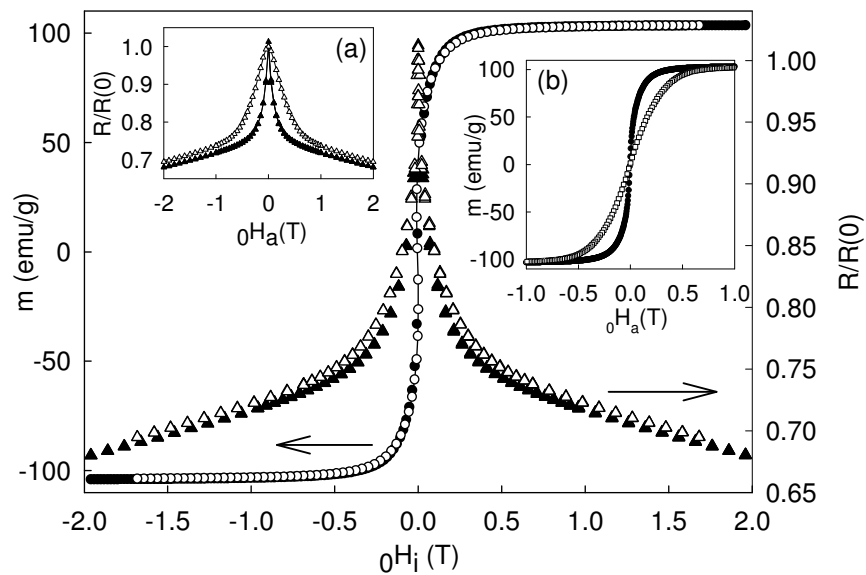
Figure 5: *Main figure: R/R(0) vs. applied magnetic field H_a curve for the S1100 sample at 20 K for perpendicular orientation: straight lines are extrapolated from the low-field and high-field regions; the intersection point is labelled (H*, RR*). Inset: RR* values plotted as a function of the temperature of the thermal treatment; black and white symbols represent samples sintered during 2 h (black) or longer (white).*
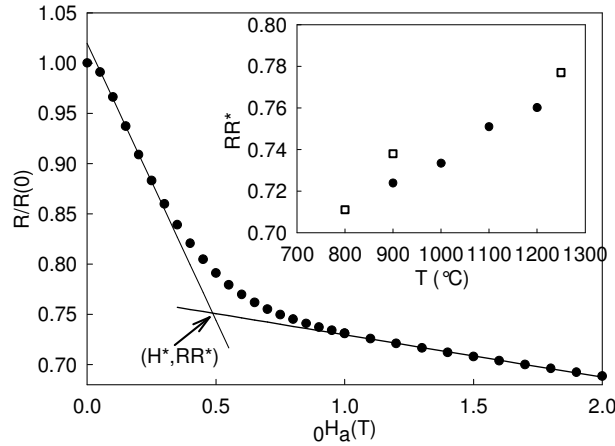

The low-field magnetoresistance effect is also influenced by the synthesis conditions. In order to compare the samples prepared at different temperatures, it was necessary to choose a parameter that is independent of the geometrical effects. Fig. 5 illustrates the procedure in the case of the S1100 sample: straight lines were extrapolated from the low-field and high-field regions of the applied magnetic field dependence of the *R/R(0)* ratio at 20 K. The intersection point of the two straight lines is labelled *(H*, RR*)*. It was shown above that the *H** value strongly depends on the sample geometry and field orientation. On the contrary the difference between the *RR** value for the two orientations turns out to be less than 0.01. In the inset of Fig. 5, the *RR** values are plotted as a function of the temperature of the thermal treatment, for perpendicular orientation of the applied magnetic field. The black and white symbols are for samples respectively sintered during 2 h or longer (see Table I for details).

It appears that the *RR** ratio increases when the temperature of the thermal treatment is increased or when the duration of the treatment is increased (inset Fig. 5). This dependence can be related to the microstructure of the samples: the samples prepared at the lowest temperatures display both a small grain size and a large low-field magnetoresistance effect. Indeed many earlier studies have shown that low-field magnetoresistance is a grain-boundary-related feature [12-14], whose origin is not yet unquestionably established [26].

The primary objective of our study was to examine the potential interest of the spray drying method for the synthesis of materials with large low-field magnetoresistance. In the inset of Fig. 5, the *RR** ratio varies between 0.711 and 0.777, or equivalently low-field magnetoresistance varies between 28.9 and 22.3% for a450°C difference of the synthesis temperature. The largest magnetoresistance is observed for the sample prepared at the lowest temperature (S800b). However, it is likely that much higher magnetoresistance ratios could have been obtained if the synthesis had been possible at temperatures below 800°C. In this respect, the occurrence of the lanthanum oxycarbonate secondary phase appears to be extremely detrimental to the optimisation of the low-field magnetoresistance properties. In order for a material to be suitable for applications, a large low-field magnetoresistance is not the only requirement: hysteresis effects should also be avoided. Fig. 6 displays the magnetic field dependences of the magnetic moment and *R/R*(0) ratio for the samples S800b and S1100. It can be seen that the sample with the largest magnetoresistance effect (S800b) shows a significant hysteresis. The good agreement between the coercive field and the positions of the maxima in the *R/R*(0) curve suggests that the hysteresis in the resistance behaviour is linked to the existence of magnetic hysteresis. Indeed, as explained by the double exchange model [5, 31], the electrical resistance of the material strongly depends on the alignment of the Mn spins, i.e., on the magnetisation. The comparison of the results for the samples S800b and S1100 in Fig. 6 shows that the coercive field increases when the synthesis temperature is decreased, i.e., when the grain size decreases. This feature is most probably related to the poorer crys-tallinity in the sample prepared at the lowest temperature (S800b): the structural disorder present in small grains, especially in the surface shell [12], is responsible for the larger irreversibility of the magnetisation curve, due to domain wall pinning by structural defects [32].

Figure 6: *Magnetic moment (left axis, black symbols) and R/R(0) ratio (right axis, white symbols) at 20 K as a function of the applied magnetic field with perpendicular orientation: (a) S800b sample and (b) S1100 sample.*
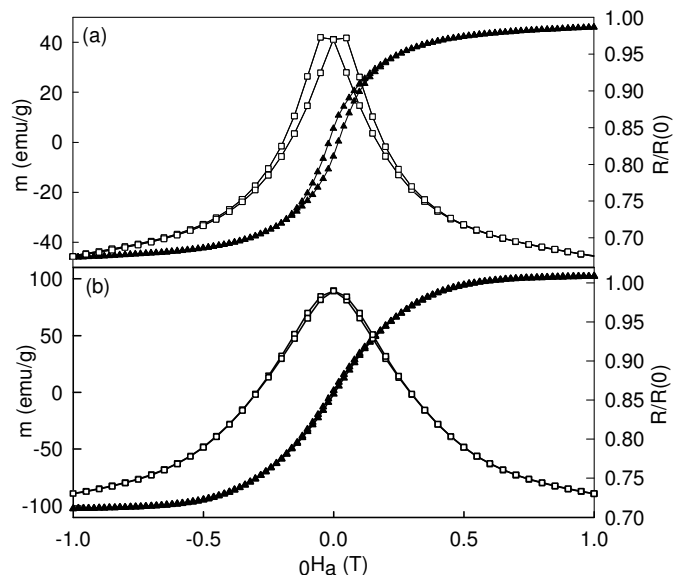
4. CONCLUSION

First of all, the present study has shown that mangan-ite compounds can be synthesised by the spray drying method. However it turns out that the synthesis of Lao.7Cao.3Mnθ3 by spray drying of an acetate solution is not suitable for the preparation of materials with very large low-field magnetoresistance effects: due to the occurrence of an intermediate phase during the decomposition of the as-sprayed powder, a rather high temperature treatment is required, to the detriment of the low field magnetoresistance. Nevertheless low-field magnetoresistance is not the only possible application of manganite compounds. The possibility to synthesise large quantities of manganites with high reproducibility has much wider interest, e.g., for applications based on the high value of the temperature coefficient of the resistivity at the resistive transition (bolometers,... [4]), or for the systematic optimisation of experimental parameters (for example during shaping or densification processes).

Beyond the spray drying issue, the results obtained during this study have also enabled us to examine the influence of the shape anisotropy (demagnetisation effects) on the magnetoresistance properties.

References

1. K. CHAHARA K, T. OHNO, T. KASAI and Y. KOZONO, *Appl. Phys. Lett.* 63 (1993) 1990.

2. R. VON HELMOLT, J. WECKER, B. HOLZAPFEL, L. SCHULTZ and K. SAMWER, *Phys. Rev. Lett.* 71 (1993) 2331.

3. Y. TOKURA, A. URUSHIBARA, Y. MORIMOTO, T. ARIMA, A. ASAMITSU, G. KIDU and N. FURUKAWA, *J. Phys. Soc. Jpn.* 63 (1994) 3931.

4. T. VENKATESAN, M. RAJESWARI, Z. W. DONG, S. B. OGALE and R. RAMESH, *Phil. Trans. R. Soc. Lond.* A 356 (1998) 1661.

5. C. N. R. RAO, A. K. CHEETHAM and R. MANESH, *Chem. Mater.* 8 (1996) 2421.

6. J. M. D. COEY, M. VIRET and S. VON MOLNAR, *Adv. Phys.* 48 (1999) 167.

7. B. RAVEAU, A. MAIGNAN, C. MARTIN and M. HERVIEU, *Chem. Mater.* 10 (1999) 2641.

8. G. J. SNYDER, R. HISKES, S. DICAROLIS, M. R. BEASLEY and T. H. GEBALLE, *Phys. Rev.* B 53 (1996) 14434.

9. R. SHREEKALA, M. RAJESWARI, K. GHOSH, A. GOYAL, J. Y. GU, C. KWON, Z. TRAJANOVIC, T. BOETTCHER, R. L. GREENE, R. RAMESH and T. VENKATESAN, *Appl. Phys. Lett.* 71 (1997) 282.

10. M. ZIESE, *Rep. Prog. Phys.* 65 (2002) 143.

11. M. SAHANA, M. S. HEGDE, C. SHIVAKUMARA, V. PRASAD and S. V. SUBRAMANYAM, ; *J. Solid State Chem.* 148 (1999) 342.

12. L. BALCELLS, B. MARTINEZ, F. SANDIUMENGE and J. F. *FONTCUBERTA, J.Magn. Magn. Mater.* 211 (2000) 193.

13. J. RIVAS, L. E. HUESO, A. FONDADO, F. RIVADULLA and M. A. LOPEZ-QUINTELA, *ibid.* 221 (2000) 57.

14. B. S. TEO, N. D. MATHUR, S. P. ISAAC, J. E. EVETTS and M. G. BLAMIRE, *J. Appl. Phys.* 83 (1998) 7157.

15. D. GANGULI and M. CHATTERJEE, "Ceramic Powder Preparation: A Handbook" (Kluwer Academic Publishers, Boston, 1997).

16. Y. LI, X. F. DUAN, J. H. ZHANG, H. R. WANG, Y. T. QIAN, Z. HUANG, J. ZHOU, S. L. YUAN, W. LIU and C. F. ZHU, *J. Mater. Res.* 12 (1997) 2648.

17. C. VAZQUEZ-VAZQUEZ, M. C. BLANCO, M. A. LOPEZ-QUINTELA, R. D. SANCHEZ, J. RIVAS and S. B. OSEROFF, *J. Mater. Chem.* 8(1998)991.

18. A. CHAKRABORTY, P. S. DEVI, S. ROY and H. S. MAITI, *J. Mater. Res.* 9 (1994) 986.

19. K. MASTERS, in "Spray Drying Handbook" (Longman Scientific and Technical, New-York, 1991).

20. G. PANNETIER, J. NATAF and A. DEREIGNE, *Bull. Soc. Chim. Fr.* (1965)321.

21. A. WOLD and R. J. ARNOTT, *J. Phys. Chem. Solids* 9 (1959) 176.

22. N. ZHANG, F. WANG, W. ZHONG and W. *DING, J. Phys.: Condens. Matter* 11 (1999) 2625.

23. R. MAHESH, R. MAHENDIRAN, A. K. RAYCHAUDHURI and C. N. R. RAO, *Appl. Phys. Lett.* 68 (1996) 2291.

24. B. VERTRUYEN, A. RULMONT, R. CLOOTS, M. AUSLOOS, S. DORBOLO and P. VANDERBEMDEN, *Mater. Lett.* 57 (2002) 598.

25. A. DE ANDRES, M. GARCIA-HERNANDEZ and J. L. MARTINEZ, *Phys. Rev.* B 60 (1999) 7328.

26. A. GUPTA and J. Z. SUN, *J. Magn. Magn. Mater.* 200 (1999) 24.

27. N. ZHANG, W. DING and W. ZHONG, *Phys. Lett.* A 253 (1999)113.

28. J. E. EVETTS, M. G. BLAMIRE, N. D. MATHUR, S. P. ISAAC, B. S. TEO, L. F. COHEN and J. L. MACMANUS-DRISCOLL, *Phil. Trans. R. Soc. Lond.* A 356 (1998) 1593.

29. J. A. OSBORN*, Phys. Rev.* 67(1945)351.

30. A. PELES, H. P. KUNKEL, X. Z. ZHOU and G. WILLIAMS, *J. Phys. Condens. Matter* 11 (1999) 8111.

31. C. ZENER*, Phys. Rev.* 82(1951)403.

32. A. K. M. AKTHER HOSSAIN, L. F. COHEN, F. DAMAY, A. BERENOV, J. MACMANUS-DRISCOLL, N. MCN. ALFORD, N. D. MATHUR, M. G. BLAMIRE and J. E. EVETTS, *J. Magn. Magn. Mater.* 192 (1999) 263.